Reactive & Functional Polymers 71 (2011) 303–314

Contents lists available at ScienceDirect

Reactive & Functional Polymers

journal homepage: www.elsevier.com/locate/react

# Inter-micellar dynamics in block copolymer micelles: FRET experiments of macroamphiphile and payload exchange

Ping Hu [a], Nicola Tirelli [b,c,*]

[a] School of Pharmacy and Pharmaceutical Sciences, University of Manchester, Oxford Road, Manchester M13 9PT, United Kingdom
[b] School of Materials, University of Manchester, Oxford Road, Manchester M13 9PT, United Kingdom
[c] School of Biomedicine, University of Manchester, Oxford Road, Manchester M13 9PT, United Kingdom

ARTICLE INFO

*Article history:*
Available online 2 November 2010

*Keywords:*
Block colymer micelles
PEG
Polysulfides
Vinyl sulfone
FRET

ABSTRACT

The co-formulation of micelles bearing different targeting groups and different payloads could allow the selective and contemporaneous treatment of various cell types with different drugs. The selectivity of such a system, however, would be compromized if macroamphiphiles and/or payloads would undergo inter-micellar exchange, homogenizing the bio-functionalization and the content of the co-formulated micelles.

Here we have investigated the occurrence of exchange phenomena in micelles of poly(propylene sulfide)–poly(ethylene glycol) (PPS–PEG) block copolymers, employing fluorophores (dansyl groups) and quenchers (dabsyl groups) either as terminal groups in macroamphiphiles or as encapsulated hydrophobic payloads. Upon exchange, the increased proximity between dansyl and dabsyl groups would significantly increase the quenching efficiency. Our results showed that even employing a rather hydrophilic block copolymer ($PPS_{10}$–$PEG_{44}$) no significant macroamphiphile exchange could be detected within 24 h from preparation. The payload exchange was temperature-dependent and could be substantially avoided for days if appropriately low storage temperatures are used.

We also present an improved experimental procedure for the synthesis of vinyl sulfone-terminated PEG and PPS–PEG and for the conjugation of these structures with labels or possibly bioactive groups.



## 1. Introduction

Micelles based on block copolymers have been extensively used as colloidal carriers for poorly water soluble molecules [1,2]. Among their distinctive advantages, they have considerably lower critical micellar concentrations (CMCs) than those of low molecular weight compounds, and therefore higher stability against dilution [3].

The self-assembly of micellar aggregates is generally based on hydrophobic association. The pioneering work of the group of Kataoka has provided a number of such systems where the associating blocks have been based e.g. on poly (β-benzyl aspartate) [4], or drug-functionalized poly(aspartic acid) [5] or poly(L,D-lactide) [6,7]. Other associative mechanisms have been used too, e.g. polyelectrolyte complexation between oppositely charged blocks, such as poly(lysine) and poly(aspartic acid) [8] or nucleic acids [9]. Among the most popular micellar systems for the solubilization of drugs, the poly(ethylene glycol)/poly(propylene glycol) di- and tri-block (Pluronics or Poloxamers) copolymers occupy a position of preminence [10,11]. The presence of poly(ethylene glycol) (PEG) ensures a prolonged circulation of Pluronic *in vivo*, but, although these polymers are non-biodegradable, the possibility of renal excretion reduces concerns about their long-term permanence [12,13]. Their relatively high CMC values, ranging between 0.01 and 10 wt.% for both di- and triblocks [1,14], appear to increase the permeation biological barriers through a double effect of unimers or poorly aggregated micelles that deplete intracellular ATP and inhibit drug efflux transporters [15,16], such as the P-glycoprotein, e.g. allowing to overcome multi-drug resistance of cancer cells [17] and allow to cross the blood–brain-barrier [18].

Polymeric micelles can be easily rendered environmentally responsive: for example, drugs can be released upon (endosomal) acidification because of the presence of pH-sensitive linkages, such as acetals [19] or Schiff bases [20,21], or because of a hydrophobic-to-hydrophilic transition of the micelle core following the protonation of aliphatic amines [22] or histidines [23]. Active biological

*Abbreviations:* PS, Propylene sulfide; TEA, Triethylamine; DBU, 1,8-Diazabicyclo undec-7-ene; TBP, Tributyl phosphine; DVS, Divinyl sulfone; PPS, Poly(propylene sulfide); PEG, Poly(ethylene glycol); DA, Dansyl; DB, Dabsyl.

* Corresponding author at: School of Materials and School of Biomedicine, University of Manchester, Oxford Road, Manchester M13 9PT, United Kingdom. Tel.: +44 1612752480.

*E-mail address:* nicola.tirelli@manchester.ac.uk (N. Tirelli).

1381-5148/$ - see front matter © 2010 Elsevier Ltd. All rights reserved.
doi:10.1016/j.reactfunctpolym.2010.10.010

targeting can been achieved through the decoration with antibodies [24], adhesion or cell-penetrating peptides [25], biotin [23], etc.

Our group has focused its attention on Pluronic-like macromolecules with a specific response to oxidation, which is obtained by replacing the Pluronic lipophilic component (poly(propylene glycol)) with the more hydrophobic poly(propylene sulfide) (PPS). PPS is hydrophobic but can be rendered hydrosoluble via oxidation of sulphur (II) to higher oxidation states [35] and this can allow for a response to the oxidative environment typical of inflammatory conditions [26–28], where the production of oxidants (e.g. Reactive Oxygen Species, ROS) is generally induced by the presence of inflammatory cytokines [29] and regulate the activity of inflammatory and phagocytic cells [30]. The cornerstone of the synthesis of PPS–PEG block copolymers is the living, anionic ring-opening polymerization of propylene sulfide. As a result of their mild character of the propagating species (thiolates) the polymerization is tolerant to a wide variety of functional groups and can even be conducted in the presence of water [31]; further, end-capping can be conveniently performed using terminal thiolates, e.g. in Michael-type additions with acrylates [32] or in substitution reactions on organic halides [33,34]. Using low MW mono- or multifunctional protected thiols (thioacetates) as initiators, and thiol-reactive PEG derivatives as end-cappers it is possible to prepare linear or star diblock structures [33,34], while PEG macroinitiators would lead to asymmetric or symmetric PEG–PPS–PEG triblock polymer structures [32]. This class of block copolymers has been used for the decoration of gold [36] or nanotube [37] surfaces, but it has also been extensively employed to generate vesicular [35,38] or micellar [34] aggregates for the encapsulation of, respectively, hydrophilic [39] or hydrophobic [40] payloads.

Here we have investigated the possibility to prepare formulations of micelles composed of identical amphiphilic polymers but bearing different payloads and surface (targeting) groups, which could address multiple cellular targets at the same time (Scheme 1); for example, it could be possible to use a single formulation to deliver a cytotoxic drug to cancer cells, an anti-inflammatory drug to inflammatory cells and a protective principle (e.g. an anti-oxidant) to normal tissue cells. In order to achieve selectivity in both targeting and delivery, however, any exchange between functional (targeting) macroamphiphiles and between payloads should be minimized.

Following the initial interpretation by Halperin and Alexander [41], the exchange of macromolecular amphiphiles between micelles is most often seen as the release of unimers in the water phase from a micelle and their uptake by a different one, a process generally referred to as the Aniansson–Wall mechanism [42]. The exchange kinetics would be essentially determined by the length of the hydrophobic block, although a retardation effect for thicker hydrophilic coronas is possible. This picture gives a central role to the equilibrium concentration of unimers, and this also implies a faster exchange for amphiphiles with higher CMC; indeed, this model provides a good description of the behavior of polymers with very hydrophobic cores, such as blocks of poly(ethylene-alt-propylene) [43–45], or poly(α-methylstyrene) [46]. However, it has also been suggested that the exchange may be in some cases dominated by events of micellar fusion and fission [47], which have also been predicted in computer simulations [48]; in this case, as reviewed by Denkova et al. [49], the concentration of block copolymer would strongly influence the exchange kinetics.

Here we have tried to develop a qualitative picture of the intermicellar exchange of both macromolecular amphiphiles and hydrophobic low molecular weight payloads by using Förster Resonance Energy Transfer (FRET, also called Fluorescence Resonance Energy Transfer). The non-radiative energy transfer between a fluorophore (a "photon donor") and a quencher (a "photon acceptor") typically shows a $1/R^6$ dependence ($R$ being the distance between fluorophore and quencher) and generally becomes negligible at distances larger than ~10 nm [50]. However, the inter-chromophoric distance for an effective quenching is proportionally larger for fluorophore/quencher couples with a substantial spectral overlap. We are interested in the co-localization of acceptor and donor groups present in different (macro)molecules, which therefore are unlikely to be in intimate contact; we have therefore chosen dansyl and dabsyl chromophores, which are characterized by an ample overlap of emission and absorption spectra. Additionally, they have good stability under irradiation and are commercially available as amine-reactive labels. The emission of dansylated amines (e.g. terminal groups on dendrimers [52] or side chains of organic polymers [53]) upon excitation in their near UV absorption band (330–340 nm) covers the spectral range between 450 and 600 nm with a maximum at about 500–520 nm in solvents from moderate-to-strong polarity (dichloromethane to water) [51], Dansyl groups have also been used as acceptors in FRET experiments, emitting upon non-radiative energy transfer from fluorophores such as ethenoadenosine [54] . More commonly, however, they have been used as FRET donors in combination with

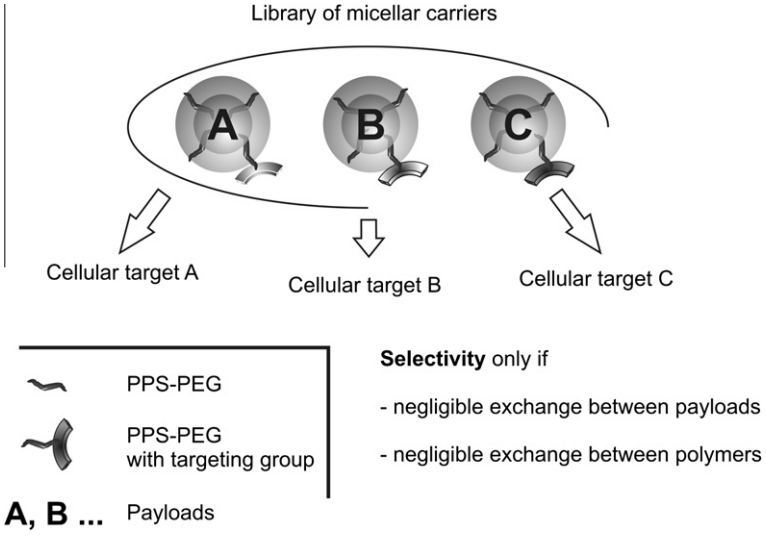


**Scheme 1.** The possibility of using a library or at least a co-formulation of identical micellar carriers differing in targeting groups and payloads could open the way to contemporaneously operate different cellular-targeted therapies. This would be possible only if exchange phenomena are minimized.

azobenzene groups, for example allowing to monitor the formation of linkages between molecular fragments [55]; for example, dansyl FRET experiments have been performed using *p*-phenylazobenzene sulfonyl (PABS) [56], 4-[(N,N-diethylamino)-phenylazo] benzene-4′-sulfonyl (DPBS) [56], 4-[4-(N,N-dimethylamino)phenylazo]-4′-benzoyl (dabcyl) [57,58] and 4-[4-(N,N-dimethylamino) phenylazo]-4′-sulfonyl (dabsyl) [57] derivatives as acceptors.

In particular, dabsyl chloride is a very stable, amine-reactive azobenzene, which was originally introduced to allow detection of peptides [59] and proteins [60] at visible light wavelengths; its push–pull structure determines a shift of the azobenzene absorption band in the visible range, thus dabsylated amines present a broad absorption in the region 370–560 nm ($\lambda_{max} \sim 430$–460 nm for dabsylated amines on polymer termini or colloidal particles [61,62]), which almost completely overlaps dansyl emission.

In order to follow the payload exchange, we have prepared dansyl and dabsyl hexylamides, as model hydrophobic payloads (Scheme 2). The macrophiphile exchange was studied reacting amine-terminated PPS–PEG derivatives with dansyl or dabsyl chloride. It is worth to notice that the macroamphiphile structure was free of cleavable groups: esters [32–35,63] or disulfides [40] have also been used as linkers, but their lability could determine the release of free or PEGylated chromophores, compromising the FRET experiments. We have therefore employed sulfone linkers, which were obtained through the Michael-type addition of thiols (PPS thiolate or cysteamine) on vinyl sulfone-terminated PEG (Scheme 2).

## 2. Experimental section

### 2.1. Materials

All materials were used as received from the supplier (Aldrich, Gillingham, United Kingdom, for acetic acid, molecular sieves, poly(ethylene glycol) diol, poly(ethylene glycol) monomethyl ether (both $\overline{M_n}$ = 2000 g/mol), propylene sulfide, sodium hydride, acetic acid, triethylamine, tributyl phosphine, divinyl sulfone, dansyl chloride, dabsyl chloride; Fluka, Gillingham, United Kingdom, for sodium methoxide solution (0.5 M in methanol), solid sodium methoxide, 1,8-diazabicyclo[5.4.0]undec-7-ene(1, 5-5)(DBU). THF was degassed by bubbling argon under inert atmosphere for 1 h before use.

### 2.2. Characterization

#### 2.2.1. Molecular characterization

$^1$H NMR spectra were recorded on 1 wt.% polymer solutions in deuterated chloroform using a 300 MHz Bruker spectrometer. FT-IR spectra were recorded in ATR mode (Golden gate) on a Tensor 27 Bruker spectrometer. GPC was performed in THF on a Polymer Laboratories GPC 50 equipped with refractive index and viscosity detectors, using universal calibration with poly(styrene) standards.

#### 2.2.2. Dynamic light scattering

Size distributions and scattering intensity of micelles were measured with the help of Zetasizer Nano ZS Instrument (Model ZEN2500, Malvern Instruments Ltd., UK). All the samples were analyzed at an angle of 114° and a temperature of 25 °C.

#### 2.2.3. Fluorescence

Fluorescent intensities of the samples were measured by a Bio-Tek Synergy 2 multi-mode microplate reader at a temperature of 25 °C (filters at excitation of 360 ± 40 nm and emission of 528 ± 20 nm).

#### 2.2.4. UV–Vis

The analyses of the UV spectra of the samples were carried out using a PerkinElmer lamda25 spectrophotometer.

### 2.3. Polymer synthesis and derivatization

#### 2.3.1. Mono-functional and di-functional end-cappers (PEG–VS and VS–PEG–VS)

The reaction was performed using variable molar ratios between monofunctional or difunctional PEG, the base (NaH) and Michael-type acceptor (DVS). Optimized conditions for the synthesis of VS–PEG–VS were as follows: 2 g (2 mmoles of OH groups) of

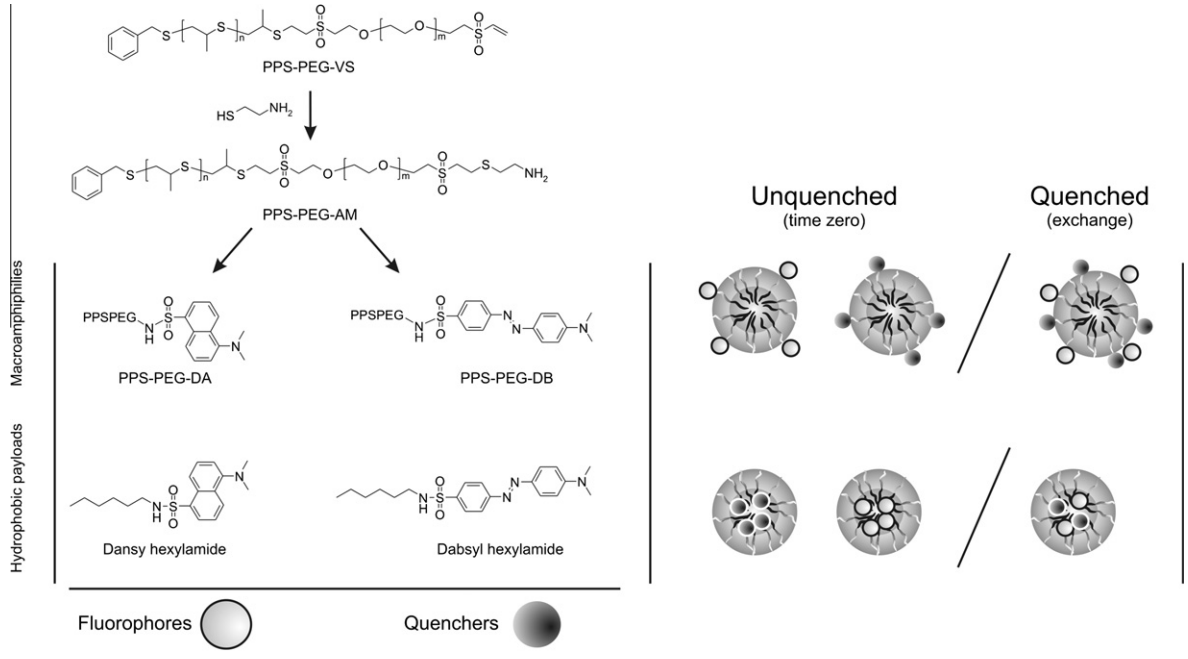


**Scheme 2.** Structures of fluorophores (dansyl derivatives) and quenchers (dabsyl derivatives) and sketch of the micellar assemblies: prior to the FRET experiments fluorophores and quenchers are present in different micellar assemblies, maximizing the fluorescence of the system; at time = $\infty$ both macroamphiphiles and payloads will equilibrate, reducing the average distance between fluorphores and quenchers and thus producing a substantial reduction to the system fluorescence.

PEG 2000 diol were dissolved in 30 mL toluene under dry nitrogen atmosphere and dried by azeotropic distillation, in a Dean–Stark apparatus, corresponding to the removal of about 10 mL of toluene. 9.6 mg of NaH (0.4 mm, corresponding to a 1:0.2 OH/NaH molar ratio) were then introduced into the reactor. When hydrogen evolution ceased, the partially deprotonated PEG solution was syphoned into another degassed reactor containing 2.96 g of DVS (25 mmoles, corresponding to 50 mmoles of double bonds, i.e. to 1:0.2:50 OH/NaH/double bond molar ratio) previously dissolved in 30 mL toluene, leaving the reaction under stirring for 24 h. The resulting mixture was filtered to remove any formed salt, neutralized adding a drop of acetic acid, reduced to small volume by rotary evaporation and finally precipitated in diethyl ester. Yield: 73% (weight of recovered polymer/theoretical amount of polymer). Conversion: 100% (molar percentage of reacted OH groups).

**FT-IR** (film on ATR crystal): **PEG–VS: 3059** ($\nu_{as}$ =$CH_2$, very weak), shoulder at 2947 ($\nu_{as}$ $CH_2$), 2855 ($\nu_s$ $CH_2$), **1639** ($\nu_s$ C=C), 1451 ($\delta_s$ $CH_2$), **1348** ($\nu_{as}$ $SO_2$), 1292, 1247, 1094 ($\nu_{as}$ C—O—C), 946, 850 $cm^{-1}$. **VS–PEG–VS: 3059** ($\nu_{as}$ =$CH_2$, very weak), shoulder at 2952 ($\nu_{as}$ $CH_2$), 2856 ($\nu_s$ $CH_2$), **1634** ($\nu_s$ C=C), 1450 ($\delta_s$ $CH_2$), **1343** ($\nu_{as}$ $SO_2$, roughly twice as intense as for PEG–VS), 1277, 1242, 1104 ($\nu_{as}$ C—O—C), 961, 839 $cm^{-1}$ (in bold the absorptions characteristic of PEG).

**$^1$H NMR** ($CDCl_3$): **PEG–VS:** $\delta$ = 3.4 (s, 3H, —OC**H$_3$**), 3.6–3.8 (broad, PEG chain protons), 6.06 (d, 1 H, C**H$_2$**=CH—$SO_2$—, cis to sulfone group), 6.22 (d, 1H, C**H$_2$**=CH—$SO_2$—, trans to sulfone group), 6.84 (d, 1 H, $CH_2$=C**H**—$SO_2$—) ppm. **VS–PEG–VS:** $\delta$ = 3.6–3.8 (broad, PEG chain protons), 6.11 (d, 2 H, C**H$_2$**=CH—$SO_2$—), 6.24 (d, 2H, C**H$_2$**=CH—$SO_2$—), 6.75 (d, 2 H, $CH_2$=C**H**—$SO_2$—) ppm.

### 2.3.2. PPS–PEG and PPS–PEG–VS block copolymers

A literature procedure based on the use of a reducing agent (TBP) during the polymerization and of a buffer containing non-nucleophilic base in the end-capping step was adopted [33]. In a typical experiment, the polymerization environment (parallel reactor FirstMate from Argonaut Technologies) was purged with nitrogen for 5 min before polymerization and 5 mL of previously degassed THF were introduced in each reactor. one milli litre of a previously degassed THF solution of S-benzyl thioacetate (containing 33.2 mg/0.2 mmol of compounds) and 1 mL of a TBP stock solution (corresponding to a 5-fold TBP: thioacetate molar ratio) were introduced in the reactor. Separately, a stock solution of sodium methoxide was prepared by mixing 380 mg of 0.5 M sodium methanoate solution in methanol (0.42 mL, 0.21 mmol, corresponding to 1.05 eq.s) with 1 mL of previously degassed THF; the solution was then added via a syringe, and the mixture was stirred at room temperature and allowed to react for 5 min. A variable quantity of PS (corresponding to 10, 20, 30 or 40 equivalents compared to thioacetate groups) was then introduced into the reactor and allowed to react for 45 min. 2 eq.s of acetic acid and 1 eq. of DBU were added to neutralize the pH. 5 mL of a THF solution containing an excess of end-capping agent (1.5 eq.s of PEG–VS for the synthesis of PPS–PEG or 10 equivalents of VS–PEG–VS polymer for the synthesis of PPS–PEG–VS) were finally added, and the mixture was stirred to react for another 2 h at room temperature.

The solvent was removed at the rotary evaporator, and the resulting viscous liquid was precipitated with ice cold diethyl ether. The oil was re-dissolved in 1 mL THF and precipitated, repeating the procedure again before transferring to water and purified through ultrafiltration using membranes with MWCO = 30,000 Da. Average yields after freeze drying: 62–88 wt.%

**FT-IR** (film on ATR crystal): **PPS–PEG: 2956** ($\nu_s$ $CH_3$), 2890 ($\nu_{as}$ $CH_2$), *2862* ($\nu_{as}$ $CH_3$ and $\nu_s$ $CH_2$), 1456 ($\delta_s$ $CH_2$), 1348 ($\nu_{as}$ $SO_2$), 1344, 1280, *1240*, **1145,** *1100* ($\nu_{as}$ C—O—C), 959, *843* $cm^{-1}$. **PPS–PEG–VS:** 3069 ($\nu_{as}$ =$CH_2$), **2957** ($\nu_s$ $CH_3$), 2881 ($\nu_{as}$ $CH_2$), *2861* ($\nu_{as}$ $CH_3$ and $\nu_s$ $CH_2$), 1649 ($\nu_s$ C=C), 1456 ($\delta_s$ $CH_2$), 1343 ($\nu_{as}$ $SO_2$), 1282, 1242, **1144,** *1100* ($\nu_{as}$ C—O—C), 961, *839* $cm^{-1}$ (in italics and underlined the absorptions characteristic of PEG, in bold those characteristic of PPS).

**$^1$H NMR** ($CDCl_3$): **PPS–PEG:** $\delta$ = 1.35–1.45 (d, $CH_3$ in PPS chain), 2.55–2.75 (m, 1 diastereotopic H of C**H$_2$** in PPS chain), 2.85–3.05 (m, C**H** and 1 diastereotopic H of C**H$_2$** in PPS chain), 3.40 (s, 3H, —OC**H$_3$**), 3.93 (t, 2H, —O—C**H$_2$**—$CH_2$—$SO_2$—), 3.6–3.8 (broad, PEG chain protons), 7.28–7.34 (m, 5H, —$CH_2$—**Ph**) ppm. **PPS–PEG–VS:** $\delta$ = 1.35–1.45 (d, $CH_3$ in PPS chain), 2.55–2.75 (m, 1 diastereotopic H of C**H$_2$** in PPS chain), 2.85–3.05 (m, C**H** and 1 diastereotopic H of C**H$_2$** in PPS chain), 3.93 (t, 4H, —O—C**H$_2$**—$CH_2$—$SO_2$—), 3.6–3.8 (broad, PEG chain protons),), 6.10 (d, 1 H, C**H$_2$** = CH—$SO_2$—), 6.24 (d, 1H, C**H$_2$**=CH—$SO_2$—), 6.81 (d, 1 H, $CH_2$=C**H**—$SO_2$—), 7.06–7.14 (m, 5H, —$CH_2$—**Ph**) ppm.

### 2.4. Synthesis of PPS–PEG–dansyl and PPS–PEG–dabsyl

150 mg of $PPS_{10}PEG_{44}$–VS (0.02 mmol of vinyl sulfone groups) and 39 mg of cysteamine. (0.2 mmol) were dissolved in 30 mL of previously degassed THF under dry nitrogen atmosphere (1:10 VS-to-thiol molar ratio). 1 mL of THF containing 5 eq.s of DBU (15.2 mg, 0.1 mmol) was then introduced dropwise into the reactor, the mixture was allowed to react for 2 h at room temperature. The THF was then evaporated and the resulting viscous syrup was precipitated in ice cold diethyl ether twice. The product was re-dissolved with 20 mL of THF and introduced into a reactor under dry nitrogen atmosphere; 2 mL of THF containing five equivalents of dansyl chloride (27 mg/0.1 mmol) or dabsyl chloride (32 mg/0.1 mmol) and triethylamine (10.1 mg/0.1 mmol) was added to the reactor. The reaction was allowed to react for 24 h with protection from light. Then the solvent was removed at the rotary evaporator and precipitated in ice cold diethyl ether twice. Yield: 57% for PPS–PEG–DA, 42% for PPS–PEG–DB. Conversion: 90% for PPS–PEG–DA, 86% for PPS–PEG–DB.

The same procedure was adopted to synthesize PEG–DB starting from PEG–VS. Yield: 66%, Conversion: 92%.

**FT-IR** (film on ATR crystal): **PPS–PEG–DA:** 3456 ($\nu_{as}$ NH), **2952** ($\nu_s$ $CH_3$), 2881 ($\nu_{as}$ $CH_2$), *2855* ($\nu_{as}$ $CH_3$ and $\nu_s$ $CH_2$), 1613, 1572 ($\nu_s$ C = C), 1470 ($\delta_s$ $CH_2$), 1358 ($\nu_{as}$ $SO_2$), 1343, 1277, 1242, **1144,** *1104* ($\nu_{as}$ C—O—C), 961, *839* ($\nu_s$ C—O—C), 793, 737 ($\omega$ =CH) $cm^{-1}$. **PPS–PEG–DB:** 3431 ($\nu_{as}$ NH), **2957** ($\nu_s$ $CH_3$), 2886 ($\nu_{as}$ $CH_2$), *2855* ($\nu_{as}$ $CH_3$ and $\nu_s$ $CH_2$), 1603, 1522 ($\nu_s$ C=C), 1450 ($\delta_s$ $CH_2$), 1419 ($\nu_s$ N=N), 1358 ($\nu_{as}$ $SO_2$), 1343, 1277, 1236, **1134,** *1104* ($\nu_{as}$ C—O—C), 961, *839* ($\nu_s$ C-O-C), 824, 686 ($\omega$ =CH) $cm^{-1}$.

**$^1$H NMR** ($CDCl_3$): **PPS–PEG–DA**: $\delta$ = 1.35–1.45 (d, $CH_3$ in PPS chain), 2.0 (s, 1H, —$CH_2$—N**H**—$SO_2$—), 2.55–2.75 (m, 1 diastereotopic H of C**H$_2$** in PPS chain), 2.85–3.05 (m, C**H** and 1 diastereotopic H of C**H$_2$** in PPS chain), 3.20 (s, 6H, N—(C**H$_3$**)$_2$), 3.43 (t, 2H, —$CH_2$—C**H$_2$**—NH—), 3.78 (t, 4H, —$SO_2$—C**H$_2$**—$CH_2$—NH—), 3.93 (t, 4H, —O—C**H$_2$**—$CH_2$—$SO_2$—), 3.6–3.8 (broad, PEG chain protons), 7.18 (d, 1H, aromatic C**H** ortho to aniline), 7.28–7.34 (m, 5H, —$CH_2$—**Ph**), 7.45–7.55 (dt, 2H, aromatic C**H** meta to aniline and meta to sulfone group), 8.22–8.38 (dd, 2H, aromatic C**H** para to aniline and para to sulfone group), 8.56 (d, 1H, aromatic C**H** ortho to sulfone group) ppm.

**PPS–PEG–DB**: $\delta$ = 1.35–1.45 (d, $CH_3$ in PPS chain), 2.0 (s, 1H, —$CH_2$—N**H**—$SO_2$—), 2.55–2.75 (m, 1 diastereotopic H of C**H$_2$** in PPS chain), 2.85–3.05 (m, C**H** and 1 diastereotopic H of C**H$_2$** in PPS chain), 3.15 (s, 6H, N—(C**H$_3$**)$_2$), 3.43 (t, 2H, —$CH_2$—C**H$_2$**—NH—), 3.78 (t, 4H, —$SO_2$—C**H$_2$**—$CH_2$—NH—), 3.93 (t, 4H, —O—C**H$_2$**—$CH_2$—$SO_2$—), 3.6–3.8 (broad, PEG chain protons), 6.78 (d, 2H, aromatic C**H** ortho to aniline), 7.28–7.34 (m, 5H, —$CH_2$—**Ph**), 7.85–7.95 (m, 4H, aromatic C**H** ortho to azo group), 8.05 (d, 2H, aromatic C**H** ortho to sulfone group) ppm.

**mPEG–DB**: $\delta$ = 2.0 (s, 1H, —$CH_2$—N**H**—$SO_2$—), 3.15 (s, 6H, N–(C**H$_3$**)$_2$), 3.4 (s, 3H, —OC**H$_3$**), 3.53 (t, 2H, —$CH_2$—C**H$_2$**—NH—),

3.78 (t, 2H, —$SO_2$—C**$H_2$**—$CH_2$—NH—), 3.93 (t, 2H, —O—C**$H_2$**—$CH_2$—$SO_2$—), 3.6–3.8 (broad, PEG chain protons), 6.78 (d, 2H, aromatic C**H** ortho to aniline), 7.28–7.34 (m, 5H, —$CH_2$—**Ph**), 7.85–7.95 (m, 4H, aromatic C**H** ortho to azo group), 8.05 (d, 2H, aromatic C**H** ortho to sulfone group) ppm.

### 2.5. Synthesis of dansyl hexylamide (DA) and dabsyl hexylamide (DB)

Under an inert atmosphere, 20 mL of dichloromethane containing 54 mg/0.2 mmol dansyl chloride or 64 mg/0.2 mmol dabsyl chloride was introduced into a parallel reactor. Then 1 mL of dichloromethane containing five equivalents of hexylamine (40 mg/1 mmol) and five equivalents triethylamine (40 mg/1 mmol) were added dropwise to the reactor. After leaving the reaction stirring for 2 h at room temperature, the resulting mixture was extracted with 20 ml of water three times to remove the salts generated by the reaction. After extraction, the organic solution was collected and concentrated by rotary evaporation and followed by further purification using silicon gel chromatography. The purified products were collected and dried, followed by verification by TLC (dichloromethane) and characterization by $^1$H NMR. The yields of the products were 51% for dansyl hexylamide and 64% for dabsyl hexylamide.

**FT-IR** (film on ATR crystal): **DA Hexylamide:** 3298 ($\nu_{as}$ NH), 2952 ($\nu_s$ $CH_3$), 2932 ($\nu_{as}$ $CH_2$), 2861 ($\nu_{as}$ $CH_3$ and $\nu_s$ $CH_2$), 1613, 1572 ($\nu_s$ C=C), 1450, 1313 ($\delta_s$ $CH_2$), 1353 ($\nu_{as}$ $SO_2$), 1160 ($\nu_s$ $SO_2$), 1139, 1068 ($\nu_s$ C—C), 961, 839 ($\nu_s$ C—O—C), 788, 732 ($\omega$ =CH) $cm^{-1}$.

**DB Hexylamide:** 3293 ($\nu_{as}$ NH), 2942 ($\nu_s$ $CH_3$), 2927 ($\nu_{as}$ $CH_2$), 2855 ($\nu_{as}$ $CH_3$ and $\nu_s$ $CH_2$), 1608, 1522 ($\nu_s$ C = C), 1450, 1323 ($\delta_s$ $CH_2$), 1419 ($\nu_s$ N=N), 1374 ($\nu_{as}$ $SO_2$), 1160 ($\nu_s$ $SO_2$), 1139, 1089 ($\nu_s$ C—C), 819, 686 ($\omega$ =CH) $cm^{-1}$.

**$^1$H NMR** ($CDCl_3$): **DA hexylamide**: $\delta$ = 0.95 (t, 3H, —$CH_2$—C**$H_3$**), 1.15 (m, 6H, —$CH_2$—(C**$H_2$)$_3$**—$CH_3$), 1.25 (m, 2H, —C**$H_2$**—($CH_2$)$_3$—$CH_3$), 2.0 (s, 1H, —$CH_2$—N**H**—$SO_2$—), 3.00 (m, 2H, —NH—C**$H_2$**—$CH_2$—), 3.15 (s, 6H, N—(C**$H_3$)$_2$**), 7.18 (d, 1H, aromatic C**H** ortho to aniline), 7.45–7.55 (dt, 2H, aromatic C**H** meta to aniline and meta to sulfone group), 8.22–8.38 (dd, 2H, aromatic C**H** para to aniline and para to sulfone group), 8.56 (d, 1H, aromatic C**H** ortho to sulfone group) ppm.

**DB hexylamide**: $\delta$ = 0.95 (t, 3H, —$CH_2$—C**$H_3$**), 1.15 (m, 6H, —$CH_2$—(C**$H_2$)$_3$**—$CH_3$), 1.25 (m, 2H, —C**$H_2$**—($CH_2$)$_3$—$CH_3$), 2.0 (s, 1H, —$CH_2$—N**H**—$SO_2$—), 3.00 (m, 2H, —NH—C**$H_2$**—$CH_2$—), 3.15 (s, 6H, N—(C**$H_3$)$_2$**), 6.78 (d, 2H, aromatic C**H** ortho to aniline), 7.85–7.95 (m, 4H, aromatic C**H** ortho to azo group), 8.05 (d, 2H, aromatic C**H** ortho to sulfone group) ppm.

### 2.7. Preparation and use of $PPS_{10}$–$PEG_{44}$ micelles

#### 2.7.1. Preparation from water

10 mL of deionized water were added to 10 mg (3.5 μmol) of $PPS_{10}$–$PEG_{44}$ at room temperature and the dispersion was stirred for 2 h.

#### 2.7.2. From organic solvents

10 mg of $PPS_{10}$–$PEG_{44}$ were dissolved in 1 mL of organic solvent (THF or DCM). This solution was added dropwise to 10 mL of deionised water under stirring and stirred at room temperature for 2 h. The organic solvent was removed by rotary evaporation (80 mbar, 25 °C, 30 min), adding water to bring the total volume to 10 mL.

### 2.8. CMC measurement

6.8 mg of pyrene were dissolved in 1 mL of THF and were further diluted to $6.7 \times 10^{-3}$ mg/mL. Then a certain amount of this diluted stock solution was added to a glass vial and the solvent was allowed to evaporate to form a thin film at the bottom of the vial. 1 mL of $PPS_{10}$–$PEG_{44}$ micelle dispersions with different concentrations ranging from 0.0001 to 10 mg/mL were added to the vial to have a final $6.7 \times 10^{-7}$ M pyrene concentration. The solutions were kept on a shaker at room temperature for 24 h to reach equilibrium prior to fluorescence measurement. Fluorescence spectra were recorded using a PerkinElmer LS55 luminescence spectrophotometer spectrometer at room temperature. Excitation wavelength: 335 nm; emission recorded at 373 nm ($I_1$) and 393 nm ($I_3$).

### 2.9. Drug loading

2 mg of DA-hexylamide or of DB-hexylamide were solubilized in 1 mL of dichloromethane. PPS–PEG micellar dispersions were prepared through direct dispersion in water as described above. 0.1 mL of the dichloromethane solutions were taken and mixed with 1 mL of the 1.0 mg/mL PPS–PEG micelle dispersion, evaporating the organic at the rotary evaporator. Any non-encapsulated payload was removed by centrifugation (solids) and dialysis (possibly over-saturated payload; MWCO = 3000 g/mol). 0.1 mL of DMF was then added to 0.1 mL of drug loaded micellar dispersion in order to disrupt the micellar aggregates and solubilize the hydrophobic compounds. The concentration of hydrophobe was then measured via its UV–Vis absorbance (DA: 340 nm, DB: 450 nm; PPS–PEG micelles have an absorbance maximum at 260 nm, with negligible absorbance at 340 or 450 nm). The concentrations of samples were calculated by comparing the readings to the standard curves of DA and DB. Hydrophobe (drug) loading (DL) and encapsulation efficiency (EE) were calculated as follows: DL (w/w) = (amount of loaded drug)/(amount of polymer), EE(wt.%) = (amount of loaded drugs)/(amount of added drugs) × 100.

### 2.10. FRET experiments

#### 2.10.1. Exchange of macroamphiphiles

In a typical experiment **(case C: DA micelles + DB micelles. Preparation from water),** 18 mg of $PPS_{10}$–$PEG_{44}$ and 2 mg of $PPS_{10}$–$PEG_{44}$–DA were dissolved in 2 mL of THF; after evaporation of the solvent at the rotary evaporator 20 mL of deionised water were added and the polymer was stirred at room temperature for 2 h. The total polymer concentration of the resulting dispersion was 1 mg/mL ($3.1 \times 10^{-4}$ M), where the concentration of $PPS_{10}$–$PEG_{44}$–DA was $3.1 \times 10^{-5}$ M (10% of overall polymer molar concentration). An identical procedure was adopted to prepare 9:1 $PPS_{10}$–$PEG_{44}$/$PPS_{10}$–$PEG_{44}$–DB dispersions in water at DB concentrations ranging between $3.1 \times 10^{-6}$ and $2.5 \times 10^{-4}$ M. 1 mL of the PPS–PEG–DB was then added to 1 mL of the PPS–PEG–DA dispersion and aliquots were transferred into a 96 well plate measuring the fluorescence emission of dansyl groups (excitation wavelength: 360 nm, emission wavelength: 528 nm) at 0, 0.5, 1, 2, 4, 16, 24 h. All measurements were conducted at 25 °C and repeated three times. In "case B" experiments, $1 \times 10^{-6}$ to $2.5 \times 10^{-4}$ M solutions of PEG–DB in water were used instead of micellar suspensions of $PPS_{10}$–$PEG_{44}$/$PPS_{10}$–$PEG_{44}$–DB. In "case A" experiments ((DA + DB) micelles), $PPS_{10}$–$PEG_{44}$ was dissolved in THF with $PPS_{10}$–$PEG_{44}$–DA and $PPS_{10}$–$PEG_{44}$–DB always in 9:1 non-labelled/labeled macroamphiphile ratio. Identical procedures were followed for the experiments on micellar suspensions prepared by diluting THF solutions in water.

#### 2.10.2. Exchange of payloads

20 mL of DA- and DB-loaded $PPS_{10}$–$PEG_{44}$ dispersions (1.0 mg/mL polymer, 0.042 mg/ml DA hexylamide, 0.034 mg/mL DB hexylamide) were prepared as described above. 2 mL of both micellar dispersions were conditioned at the target temperature (4, 25 or

37 °C), then rapidly mixed and stored in an incubator, being sampled at 0, 0.1, 0.5, 1, 2, 4, 6 h.

## 3. Results and discussion

### 3.1. Synthetic procedures

In this study, PPS–PEG amphiphilic block copolymers were prepared using a procedure based on vinyl sulfone-terminated PEG reagents. PEG vinyl sulfones have been originally proposed by Veronese as selective reagents for protein PEGylation and were obtained via reaction of PEG terminal OH groups using chloroethylsulfones as intermediates [64]. In more recent studies these groups were introduced by reacting a large excess of divinyl sulfone with an appropriate nucleophile, e.g. an *in situ* produced PEG alcoholate [65]. Such vinyl sulfone-terminated PEGs have been used to produce gels by reacting with multifunctional thiols [66,67] or to decorate nanoaggregates [68].

Here we have used this procedure to prepare mono- and later bis-vinyl sulfone-terminated PEG derivatives, optimizing the synthetic conditions reported in literature: PEG terminal OH groups were deprotonated with a stoichiometric defect (0.2 eq.s) of sodium hydride and the resulting alcoholates were reacted with a large excess of DVS (Scheme 3).

It is worth pointing out that it is necessary to use an almost catalytic amount of base to avoid parasite reactions: the Michael-type addition product is a carboanion, which can be quenched via proton transfer from protic groups (e.g. non-deprotonated alcohols), regenerating alcoholates that can carry on additional Michael-type additions. In the absence of protic groups, i.e. when stoichiometric quantities of NaH were used, viscosity sharply increased and in some cases even gelation was recorded; this is possibly due to multiple Michael-type additions on the same PEG residue and branching or cross-linking of the resulting multifunctional reagents (Scheme 3, bottom right).

For the synthesis of bis-vinyl sulfone-terminated PEG it is also necessary to employ a large stoichiometric excess of DVS, in order to avoid chain extension reactions due to double addition of alcoholates on the same sulphur centre (Fig. 1).

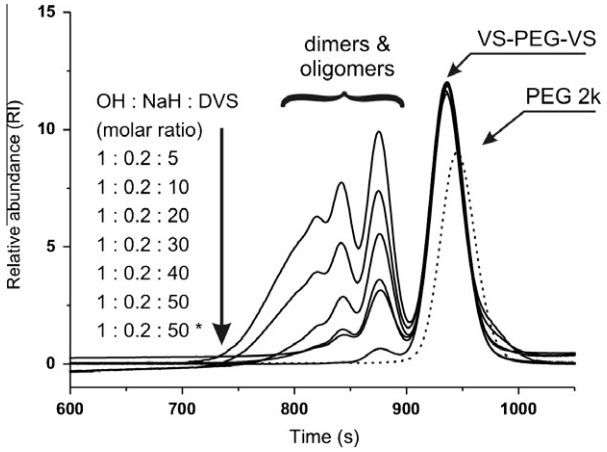


**Fig. 1.** GPC traces of the products of Michael-type addition of PEG diol (MW 2000 g/mol) on DVS obtained with a constant OH/NaH ratio and variable amounts of DVS. In most experiments DVS was added to a solution of deprotonated PEG; also at low OH/DVS molar ratios, this procedure provided significant amounts of chain extended products, e.g. about 20% of the total polymeric material for both 1:40 and 1:50 OH/DVS ratios (calculation based on the integrals of the GPC peaks). In the experiment identified as 1:0.2:50* the PEG solution was slowly dropped into a DVS solution, allowing to reduce the amount of chain extended material: the amount of dimer corresponded to less than 6% of the total polymeric material. The trace of the original PEG diol (dashed line) is reported for comparison.

The thiol-reactive PEG derivatives were then used as end-cappers to functionalize poly(propylene sulfide) chains in a *one pot* procedure comprising initiation, propagation of episulfide polymerization and end-capping of the thiol-terminated polymers; a recent review provides ample detail of the mechanism of episulfide polymerization. The optimized literature procedure is based on the use of an *in situ* deprotected initiator (in this case benzyl thioacetate), the presence of a reducing agent (tributyl phosphine) during polymerization and buffered conditions (DBU/acetic acetic acid)

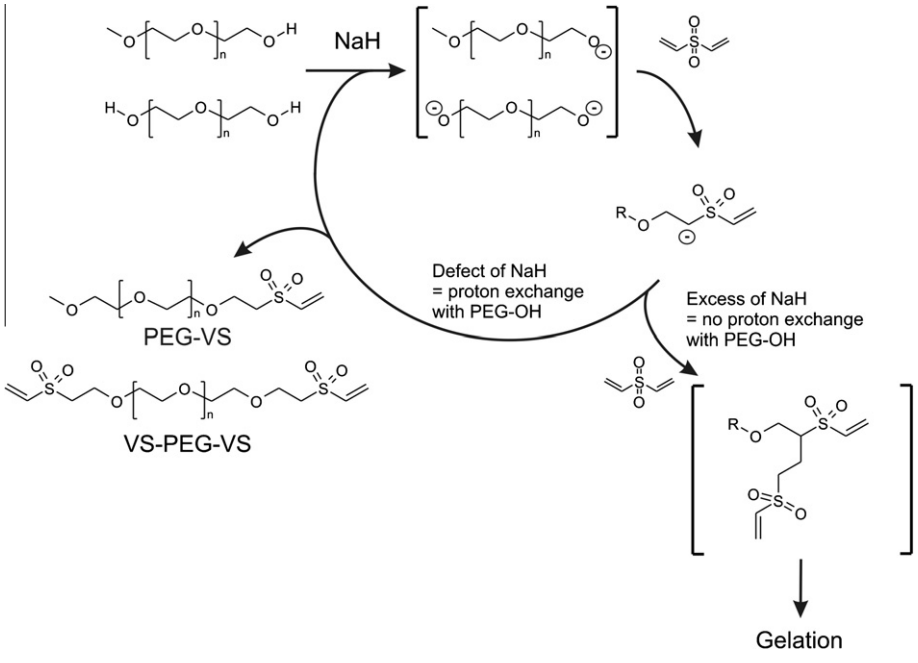


**Scheme 3.** Functionalization of monomethoxy PEG and PEG diol with terminal vinyl sulfone groups. NaH was employed in stoichiometric defect to the PEG OH groups (typically 20% in moles), since the Michael-type addition product can on its turn deprotonate OH groups and re-initiate the reaction. When it was used in excess, gelation occurred, possibly because of formation of multifunctional derivatives.

for the end-capping, to avoid disulfide formation and side-reactions on the vinyl sulfone groups due to the use of excess base [63].

All polymers were characterized by quantitative end-capping and narrow molecular weight distribution. (Fig. 2 and Table 1).

Finally, the labeled polymers were prepared by reacting vinyl sulfone-terminated macromolecules first with cysteamine and then with the amine-reactive dansyl or dabsyl chloride, as depicted in Scheme 2.

### 3.2. Preparation and drug loading of non-functional PPS–PEG micelles

In a recent paper by Velluto et al. [40], PPS–PEG micelles have been produced and loaded with cyclosporine A using polymers ($PPS_{10}$–$PEG_{44}$, $PPS_{20}$–$PEG_{44}$ and $PPS_{30}$–$PEG_{44}$) with only very minor differences from those prepared in this study: those structures had no sulfone linking PPS and PEG blocks and a thiopyridine PPS terminal group where we have used a benzylic group; in addition, the polymerization conditions adopted in that reference are more prone to the formation of PPS homopolymer due to disulfide-mediated chain transfer [63,69].

Since these differences do not seriously affect the hydrophilic/lipophilic balance of the polymers, the aggregates of the polymers produced in this study show a substantially identical size to those previously reported, with a *Z*-average size of 20–23 nm for $PPS_{10}$–$PEG_{44}$ and $PPS_{20}$–$PEG_{44}$, 24–27 nm for $PPS_{30}$–$PEG_{44}$, and a bimodal and broad distribution for $PPS_{40}$–$PEG_{44}$, (Fig. 3A) which has already been demonstrated to form also larger aggregates, such as worm-like micelles and vesicles [40]. It is worth mentioning that the above diameters refer to micelles prepared by stirring PPS–PEG polymers in deionized water at room or higher temperature; differently from the results reported by Velluto et al., the dispersion of dichloromethane or THF solutions in water followed by the evaporation of the solvent provided considerably larger aggregates (Fig. 3B), which are possibly formed by clustered/entangled micelles.

The Critical Aggregation Concentrations showed a clear dependence on the length of PPS block (Fig. 3C and D), which in our case are 2–5 smaller than in the work of Velluto et al. (Table 1, last column). Since the same analytical method was used, these discrepancies are likely to be ascribed to the small structural differences of the polymers (PPS terminus pyridine vs. benzyl group; PEG–PPS junction ether vs. sulfone).

We have then used the two model hydrophobic compounds prepared in this study (dansyl hexyl hexylamide and dabsyl hexylamide) to evaluate the loading capacity of the PPS–PEG micelles as a function of the PPS length (Table 2). For both compounds the loading and the encapsulation efficiency increased with increasing PPS length for degrees of polymerization 10 to 30. The performance of $PPS_{40}$–$PEG_{44}$ is apparently poorer, but we are inclined to consider this to be an artefact caused by the partial sedimentation of $PPS_{40}$–$PEG_{44}$ large aggregates, when the dispersions were centrifuged to remove any non-encapsulated drug in crystalline form.

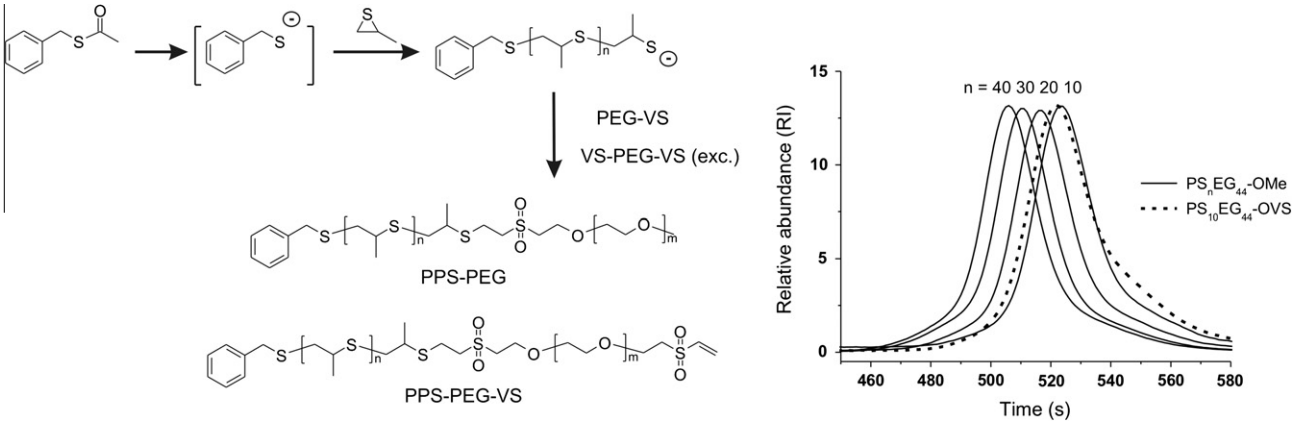


**Fig. 2.** *Left:* a benzyl mercaptane anion was generated *in situ* from the corresponding thioacetate and used to initiate the ring-opening polymerization of propylene sulfide. The resulting thiolate-terminated macromolecules were then end-capped with PEG–VS (used stoichiometrically) or VS–PEG–VS (used in large excess). *Right:* The sequence of reactions always provided polymers with monomodal MW distribution and low polydispersity.

**Table 1**
Summary of the characterization data for PEG and PPS–PEG derivatives.

| Sample | End-capping conversion (% mol)[a] | Yield (wt.%)[b] | Theor. DP of each PPS arm[c] | NMR $\overline{M_n}$[d] | GPC[e] $\overline{M_n}$ | $\overline{M_w}/\overline{M_n}$ | CAC[f] (mg/mL) |
|---|---|---|---|---|---|---|---|
| $PEG_{44}$–VS | 100 | 78 | n.a. | 2100 | 2400 | 1.05 | n.a. |
| VS–$PEG_{44}$–VS | 100 | 73 | n.a. | 2200 | 2600 | 1.08 | n.a. |
| $PPS_{10}PEG_{44}$ | 95 | 88 | 10 | 2900 | 3400 | 1.15 | 0.185 (0.392[40]) |
| $PPS_{20}PEG_{44}$ | 93 | 85 | 20 | 3600 | 4200 | 1.16 | 0.130 (0.350 [40]) |
| $PPS_{30}PEG_{44}$ | 94 | 78 | 30 | 4600 | 5300 | 1.08 | 0.031 |
| $PPS_{40}PEG_{44}$ | 93 | 81 | 40 | 5400 | 6100 | 1.14 | 0.011 (0.052 [40]) |
| $PPS_{10}PEG_{44}$–VS | 94 | 62 | 10 | 3000 | 3300 | 1.11 | = |
| $PPS_{10}PEG_{44}$–DA | 90 | 57 | 10 | 3200 | 3400 | 1.15 | = |
| $PPS_{10}PEG_{44}$–DB | 86 | 42 | 10 | 3300 | 3600 | 1.17 | = |

[a] Calculated from the ratio of the $^1$H NMR resonance of PEG terminal groups ($CH_3$ at 3.4 ppm or vinyl sulfone at 6.1–6.2 ppm) and the resonance of PEG main chain for the PEG–VS and VS–PEG–VS, or that of the aromatic group of the initiator (7.4 ppm) for the other polymers.
[b] Weight of recovered polymer/weight of monomer + deprotected initiator + stoichiometric amount of PEG derivative.
[c] Theoretical degree of polymerization (DP), expressed as the ratio [PS]/[thiol].
[d] From the ratio of the $^1$H NMR resonance of the PPS $CH_3$ group (1.4 ppm) of the aromatic group of the initiator (7.4 ppm).
[e] Calculated from GPC data in THF by the means of the universal calibration with poly(styrene) standards and viscosimetric and RI detection.
[f] In brackets data from Ref. [40]. The CACs for the functional derivatives of $PPS_{10}PEG_{44}$ were assumed identical to those of $PPS_{10}PEG_{44}$.

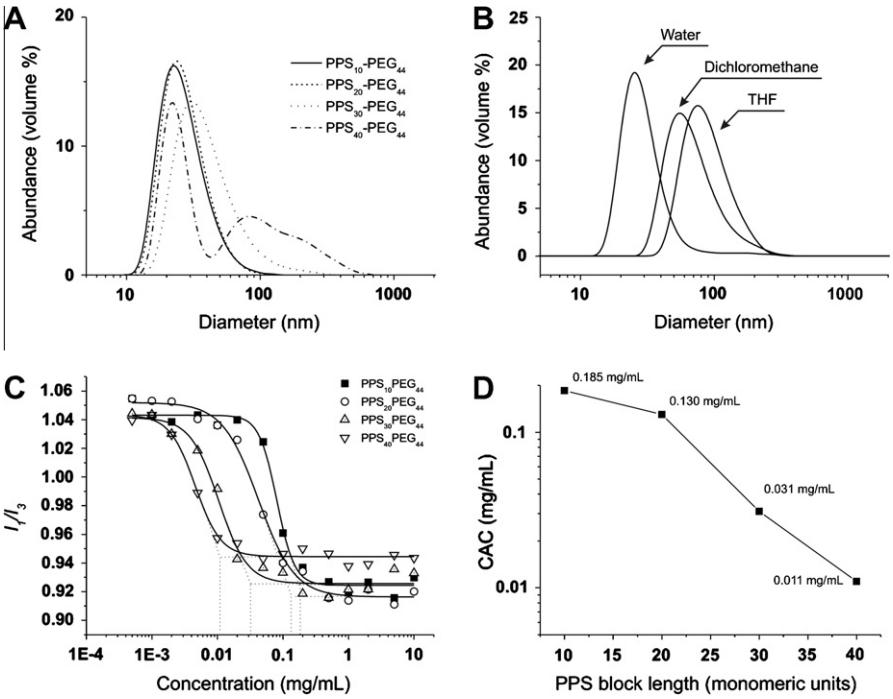


**Fig. 3.** (A) Size distributions of micelles of $PPS_{10}$–$PEG_{44}$ to $PPS_{40}$–$PEG_{44}$. The dispersions were prepared at room temperature directly in water. (B) Influence of the preparation method on the size of the micelles; the presence of organic solvents shifted the size distribution to larger values. (C) *I1/I3* Emission ratio for pyrene as a function of the polymer concentration; the lines represent sigmoidal (Hill) fits of the experimental points; the CACs were determined as the end point of the sigmoids as indicated by dashed lines in the figure. (D) Dependence of the CAC on the degree of PS degree of polymerization; although the CAC values have been reported with a logarithmic scale, there are too few data points to highlight a logarithmic relation between the two variables.

**Table 2**
Loading and encapsulation efficiency for the two hydrophobic reporters (drugs) in PPS–PEG micellar dispersions[a].

| Polymer | DA | | DB | |
|---|---|---|---|---|
| | Drug loading[b] (mg/mg) | Encapsulation efficiency[c] (wt.%) | Drug loading[b] (mg/mg) | Encapsulation efficiency[c] (wt.%) |
| $PPS_{10}PEG_{44}$ | 0.0422 ± 0.008 | 21.1 ± 4.0 | 0.0344 ± 0.002 | 17.2 ± 1.1 |
| $PPS_{20}PEG_{44}$ | 0.0637 ± 0.007 | 31.9 ± 3.6 | 0.0449 ± 0.007 | 22.5 ± 3.6 |
| $PPS_{30}PEG_{44}$ | 0.0931 ± 0.009 | 46.6 ± 4.6 | 0.0694 ± 0.008 | 34.7 ± 3.8 |
| $PPS_{40}PEG_{44}$ | 0.0799 ± 0.006 | 39.9 ± 3.2 | 0.058 ± 0.006 | 29.4 ± 3.1 |

[a] Polymer concentration: 1 mg/mL; 1:5 drug/polymer weight ratio.
[b] Amount of drug loaded/amount of polymer.
[c] Amount of drug loaded/total amount of drug used * 100.

For further studies we have focused our attention on $PPS_{10}$–$PEG_{44}$: its high hydrophilic content makes it the polymer with possibly the quickest inter-micellar exchange kinetics and therefore the "worst case" scenario candidate. However, although characterized by the smallest PPS content, $PPS_{10}$–$PEG_{44}$ still showed a well-defined molecular structure (low polydispersity) and micellar organization (no large aggregates, rather low CAC and therefore good stability against dilution) and a reasonable drug loading.

Finally, it is worth noting that the size of the micelles formed by vinyl sulfone-terminated $PPS_{10}$–$PEG_{44}$ or its labeled derivatives, alone or in mixture with non-functional $PPS_{10}$–$PEG_{44}$, was indistinguishable from that of $PPS_{10}$–$PEG_{44}$-only micelles (Fig. 4). This ensures that the presence of the chromophores did not significantly alter the micellar self-assembly of PPS–PEG.

### 3.4. FRET experiments

#### 3.4.1. Exchange between macroamphiphiles

Spatial proximity is the major determinant of the quenching efficiency of dansyl emission. Here we have considered three possible situations (Scheme 4), employing $PPS_{10}$–$PEG_{44}$ at a concentration at least one order of magnitude higher than its CMC:

*Case A:* (DA + DB) micelles, i.e. micelles prepared from premixed DA- and DB-labelled PPS–PEG polymers (intra-micellar quenching). This situation forces the closest proximity between the chromophores while hydrophobic aggregation boosts the local concentration of both, therefore it is expected quenching (expressed as FRET efficiency, $\varepsilon$) to be maximal. We also expect it to increase with increasing DB/DA ratio and not to depend on time, since any exchange between micelles will not alter the average DB/DA ratio.

*Case B:* DA micelles + PEG–DB, i.e. micelles containing PPS–PEG–DA exposed to a hydrophilic polymeric quencher, PEG–DB (interfacial quenching). Since PEG–DB lacks of a hydrophobic anchor, (a) FRET to DB could only take place on the micellar surfaces; (b) the DB concentration in proximity to DA would be considerably smaller than in case A. As a result, the quenching efficiency should be strongly limited; however, as above, quenching should significantly depend on the PEG–DB concentration and, since exchange phenomena are impossible, also in this case we expect to observe no time dependence.

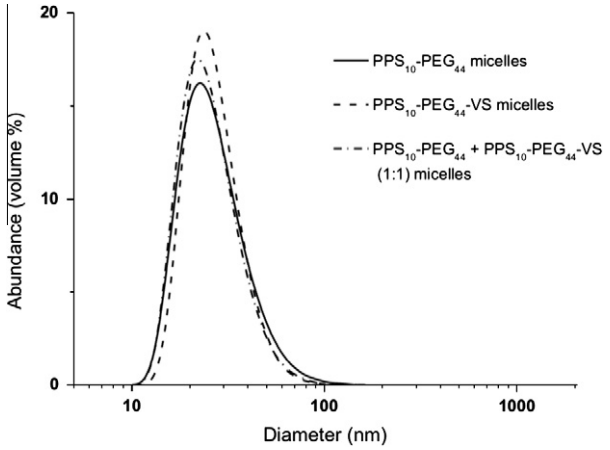


**Fig. 4.** The size the micellar aggregates is not influenced by the replacement of the terminal methoxy group of $PPS_{10}$–$PEG_{44}$, with the vinyl sulfone of $PPS_{10}$–$PEG_{44}$–VS; identical distributions are obtained for the polymers independently or in 1:1 M mixture.

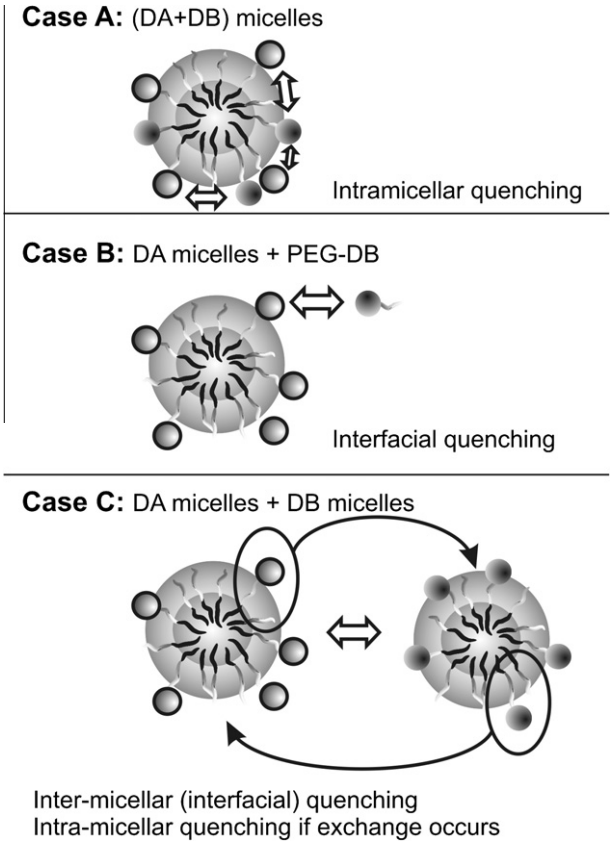


**Scheme 4.** FRET experiments aiming at assessing the exchange of PPS–PEG macroamphiphiles between micelles were conducted on three different systems: (A) micelles containing both FRET donor and acceptor, where any quenching would be predominantly intra-micellar. (B) Donor (DA)-containing micelles exposed to a solution of PEGylated acceptor, where any quenching would be predominantly interfacial, since PEG–DB cannot get anchored in the micellar core. (C) Donor-containing micelles and acceptor-containing ones mixed together, where the quenching could be time-dependent and intra-micellar when exchange occurs appreciably, or predominantly interfacial when it does not.

*Case C:* DA micelles + DB micelles, i.e. micelles separately prepared from PPS–PEG–DA and PPS–PEG–DB (inter- or intra-micellar quenching). Two cases are given: (1) if no rapid exchange between macroamphiphiles occurs, the FRET efficiency does not depend on time, as in cases A and B. Quenching is likely to be higher than in case B, because DB is present in micellar aggregates and therefore its local concentration is higher than its macroscopic one. However, FRET should be less intense than in case A, due to the less intimate contact between fluorophore and quencher. (2) If exchange occurs, quenching efficiency should increase with time. The dependence of quenching on DB concentration may show a similarity to case B at shorter times (interfacial quenching) while becoming similar to case A at longer ones (intra-micellar quencher).

We have investigated PPS–PEG micelles produced both by directly dispersing the polymers in water and by diluting in water a THF solution, i.e. in the two cases of smaller and larger micellar aggregates. In all cases the micelles were composed of unlabelled macroamphiphiles in a 9-fold molar excess of labelled PPS–PEG, in order to avoid self-quenching effects of the fluorophores.

Fig. 5 reports The FRET efficiency as a function of the quencher concentration and time for the three cases reported above for both aggregates produced from THF solutions (size 50–110 nm; Fig. 5 top row) and those obtained through direct dispersion of the polymers in water (size 20–30 nm; Fig. 5 bottom row). It is immediately apparent that all systems exhibited a rather flat time dependence, and an asymptotic dependence on DB concentration.

A closer look at the time dependence (1:1 DA/DB molar ratio; Fig. 6, left graphs) confirms that in all cases FRET efficiency was substantially constant for at least 24 h. A small increase in quenching is recorded within the first hour after mixing; however, since this is also recorded for pre-mixed macroamphiphiles, it cannot be related to exchange phenomena. The above is therefore a first indication of the absence of rapid inter-micellar exchange between macroamphiphiles. At all time points the FRET efficiency was in the order case A (pre-mixed polymers: (DA + DB) micelles) > case C (DA micelles + DB micelles) > case B (DA micelles + PEG–DB), indicating the absence of intra-micellar quenching in case C, which otherwise would increase to the level of case A.

It is also noteworthy that the quenching shown by large aggregates was significantly, although not dramatically higher than that of smaller ones; this was more clear for case A ((DA + DB) micelles) and case B (DA micelles + PEG–DB). The large aggregates are possibly characterized by a less compact packing and therefore by a quicker internal dynamics, which may allow more intimate contact between fluorophores and quenchers.

The differences between the three cases and in particular the intermediate behavior of case C were quantified using the dependence of FRET efficiency on DB concentration at 0.5 h after mixing (Fig. 6, right graphs). The data points were fitted with a double exponential model $\varepsilon([DB]) = \varepsilon_{\infty} - \varepsilon_{low} \exp(-[DB]/S_{low}) - \varepsilon_{high} \exp(-[DB]/S_{high})$; $S_{low}$ and $S_{high}$ $B$ are in the essence the slopes of the curves at low and high DB concentration, respectively. The curves showed strong similarities at large DB concentration, with $S_{high} \sim 1$ L/mmol, indicating that at millimolar or higher concentrations FRET happens similarly disregarding the physical organization of the chromophores. The parameter $S_{low}$, on the other hand, showed a clear trend increasing from about 0.1 L/mmol for case B (interfacial quenching) to 0.03 L/mmol for case A (intra-micellar quenching.

The intermediate behavior of case C in terms of FRET efficiency and of its dependence on concentration, and the absence of a sound time dependence within the first 24 h have therefore led us to conclude that no rapid amphiphile exchange occurs between $PPS_{10}$–$PEG_{44}$ micelles.

### 3.4.2. Exchange between payloads

DA hexylamide and DB hexylamide were employed as model hydrophobic payloads and separately loaded in micellar suspensions of unlabelled $PPS_{10}$–$PEG_{44}$ (1 mg/mL polymer in both cases, 0.042 mg/mL DA, 0.034 mg/mL DB); the two suspensions were

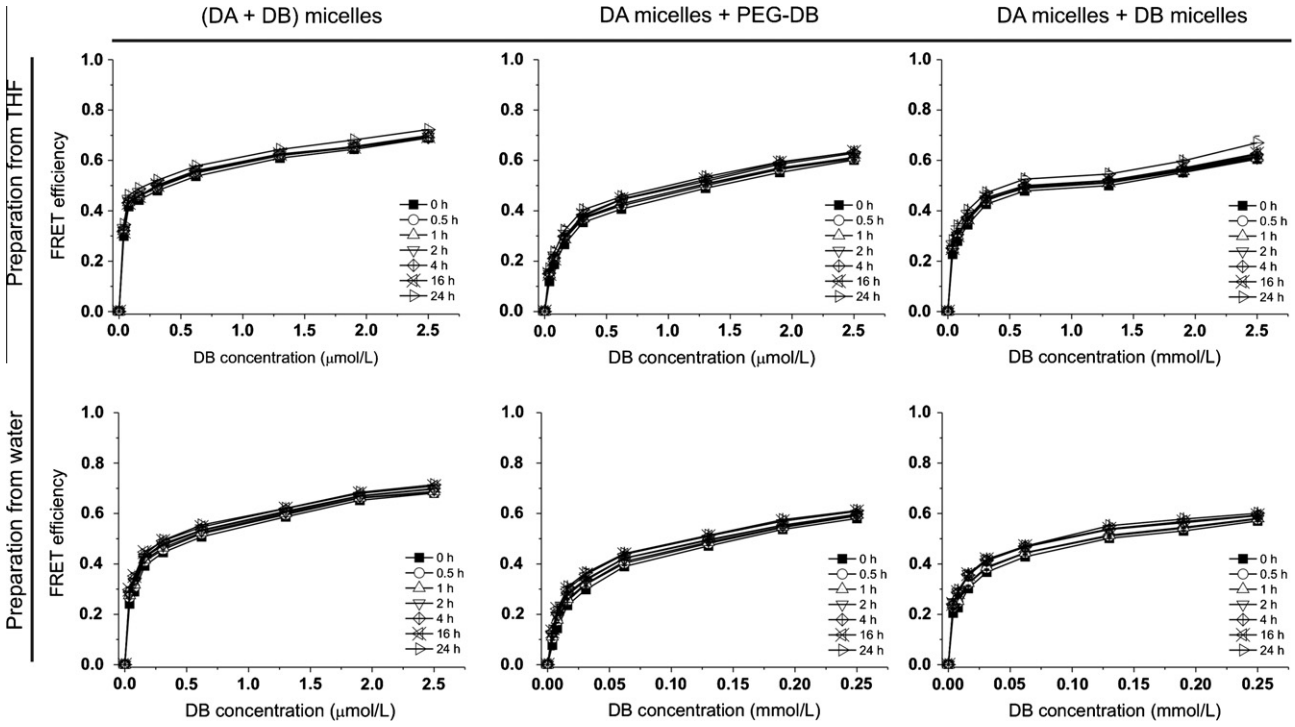


**Fig. 5.** FRET efficiency (=1 – normalized fluorescence) as a function of the molar concentration of DB groups in the three cases of DB- and DA-terminated PPS–PEG pre-mixed and then dispersed in micelles (case A), of PPS–PEG–DA micelles exposed to PEG–DB (case B),and of PPS–PEG–DA and PPS–PEG–DB first dispersed in micelles and then mixed together (case C). The DA concentration was kept constant to $3.1 \times 10^{-5}$ M and the ratio between labeled and un labelled polymer was kept constant to 1:10. All data are averages over three measurements. *Top row*: aggregates produced via dilution in water of a THF solution. *Bottom row*: aggregates produced via direct dispersion of the bulk polymers in water.

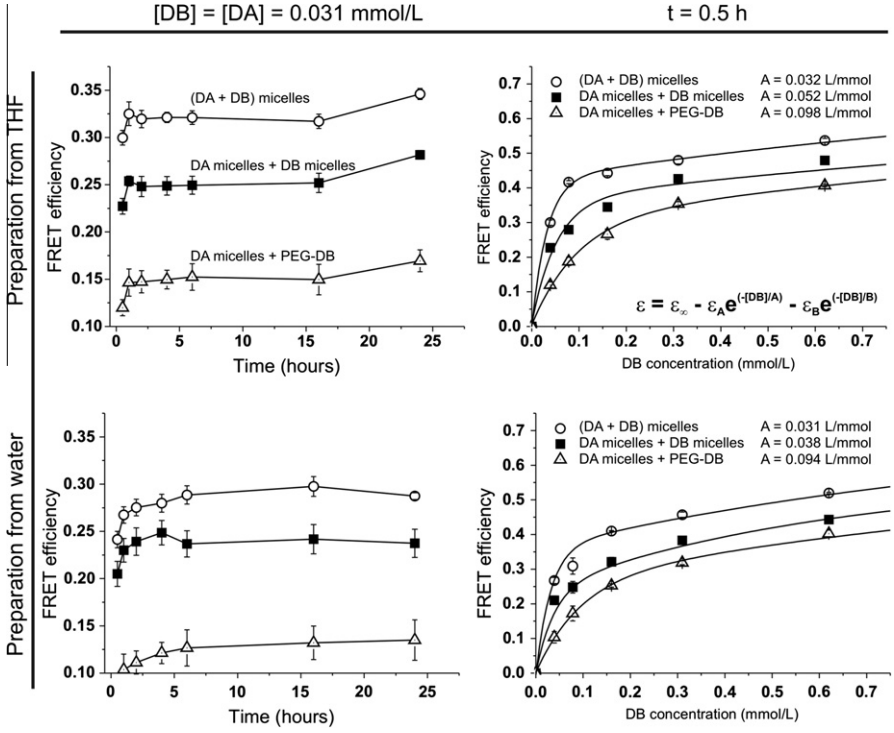


**Fig. 6.** *Left:* FRET efficiency as a function of time for PPS–PEG–DA micelles with a DA concentration = $3.1 \times 10^{-5}$ M (1 mg/mL $PPS_{10}$–$PEG_{44}$ concentration, 10% of it labeled with DA) and prepared by diluting a concentrated THF solution (*Top*) or directly dispersing the polymer in water (*Bottom*) exposed to equimolar amounts of DB initially present in the same micelles (white circles), in different micelles prepared in identical fashion (black squares) or in solution (white triangles). *Right:* Dependence of the FRET efficiency (time = 0.5 h after mixing) on DB concentration for micelles prepared from a THF solution (*Top*) or via direct dispersion in water (*Bottom*), same concentration as above. The solid lines represent the result of a double exponential fit; the values of the characteristic parameter A (i.e. the slope of the initial part of the curves) are reported.

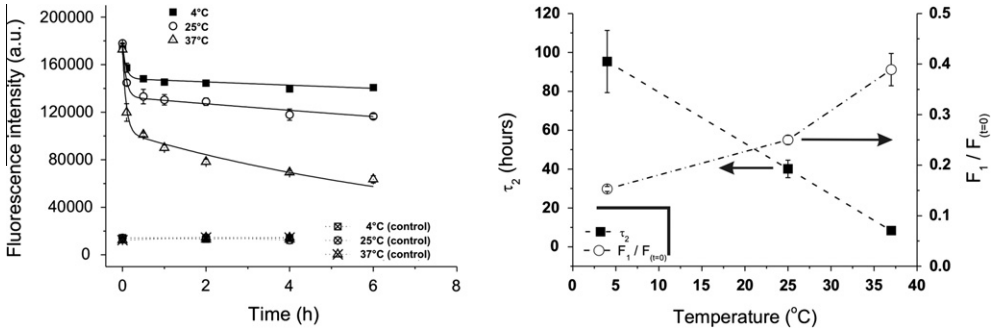


**Fig. 7.** *Left:* Fluorescence intensity of DA-loaded PPS–PEG micelles as a function of time and temperature upon exposure to DB-loaded PPS–PEG micelles (1:1 DB/DA molar ratio). Micelles loaded with pre-mixed hydrophobes (same molar ratio) were used as controls. The solid lines represent the results of fittings using a model of biexponential decay. *Right:* The relative amount of "instantaneous" quenching ($F_1/F_{t=0}$) increases with temperature, possibly due to the increased DB hexylamide solubility in water; the characteristic time of the slower quenching component ($\tau_2$) decreases with temperature, due to accelerated inter-micellar diffusion.

then mixed together in 1:1 weight ratio, in order to obtain a roughly 1:1 DA/DB molar ratio, while micelles loaded with the two drugs (1:1 M ratio) were used as a control. DA fluorescence was then monitored as a function of time and temperature (Fig. 7), providing information on the kinetics of exchange of DB.

The fluorescence intensity exhibited a clear biexponential behavior, which we have modeled as, $F(t) = F_\infty - F_1 \exp(-t/\tau_1) - F_2 \exp(-t/\tau_2)$, where $F_\infty$ is the fluorescence intensity of the controls (Fig. 7, left). The first phase is an almost instantaneous quenching, whose characteristic time ($\tau_1 < 3$ min) does not appear to have a sound dependence on temperature, while the corresponding extent of quenching ($F_1/F_{t=0}$) increases with increasing temperature. Since DB solubility will increase with temperature, we are inclined to ascribe this phase to the action of DB in solution, occurring immediately after mixing and without penetration in the micellar cores. This is then followed by a slower phase, where the characteristic time ($\tau_2$) shows the expected temperature dependence (Fig. 7, right).

The results obtained for DB hexylamide indicate a substantial payload exchange in a few hours at 37 °C; however, this phenomenon is considerably retarded at 4 °C, and at this temperature the payload exchange appears negligible for the first day(s) after preparation. These data are payload-specific and, furthermore, they also depend on the concentration of both micellar carrier and payload; however, as a general indication it appears that storage at cold temperature could allow for a reasonably long storage of a micellar co-formulation with different payloads. On the other hand, the permanence at body temperature may be a critical point and the efficacy of a micellar library will strongly rely on the efficiency of the targeting groups.

## 4. Conclusions

This study has provided a semi-quantitative assessment of inter-micellar exchange phenomena occurring in PPS–PEG dispersions. We have selected a polymer with a rather small hydrophobic tail, $PPS_{10}$–$PEG_{44}$. Its predominantly hydrophilic structure should provide the quickest exchange rate within an Aniansson–Wall mechanism; the relatively high concentration (1 mg/mL) used should also boost exchanges through micellar fusion and fission. Our FRET experiments have used two control systems: as expected, significant differences were recorded between the quenching efficiency in the three cases of fluorophore + quencher in the same micelle (maximum quenching), in different micelles (intermediate quenching) and fluorophore in micelle + quencher in solution (lowest quenching). However, in no case we have recorded a clear time dependence, which suggests no rapid macroamphiphile exchange to take place with either mechanism.

FRET experiments between payloads have shown a quicker dynamics (at room or body temperature) in comparison to the macroamphiphiles, which is possibly to be ascribed to the higher solubility in the water medium. However, it is also possible to substantially slow down the payload exchange at low temperature.

In the perspective of co-formulating differently functional and differently loaded micellar carriers, our results suggest that such preparations could be stored for relatively long periods (days) at low temperature and may have a life time of a few hours at body temperature, requiring therefore a relatively quick targeting action.

## References

[1] A.V. Kabanov, E.V. Batrakova, N.S. Meliknubarov, N.A. Fedoseev, T.Y. Dorodnich, V.Y. Alakhov, V.P. Chekhonin, I.R. Nazarova, V.A. Kabanov, J. Control. Release 22 (1992) 141–157.
[2] V.P. Torchilin, Cell. Mol. Life Sci. 61 (2004) 2549–2559.
[3] V.P. Torchilin, J. Control. Release 73 (2001) 137–172.
[4] G. Kwon, M. Naito, M. Yokoyama, T. Okano, Y. Sakurai, K. Kataoka, Langmuir 9 (1993) 945–949.
[5] M. Yokoyama, M. Miyauchi, N. Yamada, T. Okano, Y. Sakurai, K. Kataoka, S. Inoue, Cancer Res. 50 (1990) 1693–1700.
[6] Y. Nagasaki, T. Okada, C. Scholz, M. Iijima, M. Kato, K. Kataoka, Macromolecules 31 (1998) 1473–1479.
[7] Y. Yamamoto, Y. Nagasaki, Y. Kato, Y. Sugiyama, K. Kataoka, J. Control. Release 77 (2001) 27–38.
[8] A. Harada, K. Kataoka, Macromolecules 28 (1995) 5294–5299.
[9] S. Katayose, K. Kataoka, Bioconjucate Chem. 8 (1997) 702–707.
[10] A.V. Kabanov, E.V. Batrakova, V.Y. Alakhov, J. Control. Release 82 (2002) 189–212.
[11] D.A. Chiappetta, A. Sosnik, Eur. J. Pharm. Biopharm. 66 (2007) 303–317.
[12] E.V. Batrakova, S. Li, Y.L. Li, V.Y. Alakhov, W.F. Elmquist, A.V. Kabanov, J. Control. Release 100 (2004) 389–397.
[13] J.M. Grindel, T. Jaworski, O. Piraner, R.M. Emanuele, M. Balasubramanian, J. Pharm. Sci. 91 (2002) 1936–1947.
[14] D. Attwood, C. Booth, S.G. Yeates, C. Chaibundit, N. Ricardo, Int. J. Pharm. 345 (2007) 35–41.
[15] E.V. Batrakova, S. Li, S.V. Vinogradov, V.Y. Alakhov, D.W. Miller, A.V. Kabanov, J. Pharmacol. Exp. Ther. 299 (2001) 483–493.
[16] E.V. Batrakova, S. Li, Y.L. Li, V.Y. Alakhov, A.V. Kabanov, Pharm. Res. 21 (2004) 2226–2233.
[17] T. Yamagata, H. Kusuhara, M. Morishita, K. Takayama, H. Benameur, Y. Sugiyama, J. Control. Release 124 (2007) 1–5.
[18] E.V. Batrakova, D.W. Miller, S. Li, V.Y. Alakhov, A.V. Kabanov, W.F. Elmquist, J. Pharmacol. Exp. Ther. 296 (2001) 551–557.
[19] E.R. Gillies, J.M.J. Frechet, Bioconjucate Chem. 16 (2005) 361–368.
[20] Y. Bae, N. Nishiyama, S. Fukushima, H. Koyama, M. Yasuhiro, K. Kataoka, Bioconjucate Chem. 16 (2005) 122–130.
[21] H.S. Yoo, E.A. Lee, T.G. Park, J. Control. Release 82 (2002) 17–27.
[22] Y.Q. Tang, S.Y. Liu, S.P. Armes, N.C. Billingham, Biomacromolecules 4 (2003) 1636–1645.
[23] E.S. Lee, K. Na, Y.H. Bae, Nano Lett. 5 (2005) 325–329.
[24] V.P. Torchilin, A.N. Lukyanov, Z.G. Gao, Proc. Natl. Acad. Sci. USA 100 (2003) 6039–6044.
[25] X.B. Xiong, H. Uludag, A. Lavasanifar, Biomaterials 31 5886-5893.

[26] J. Emerit, A. Edeas, F. Bricaire, Biomed. Pharmacother. 58 (2004) 39–46.
[27] T.M. Paravicini, R.M. Touyz, Diabetes Care 31 (2008) S170–S180.
[28] F. Bonomini, S. Tengattini, A. Fabiano, R. Bianchi, R. Rezzani, Histol. Histopathol. 23 (2008) 381–390.
[29] Y.S. Kim, M.J. Morgan, S. Choksi, Z.G. Liu, Mol. Cell 26 (2007) 675–687.
[30] L. Fialkow, Y.C. Wang, G.P. Downey, Free Rad. Bio. Med. 42 (2007) 153–164.
[31] A. Rehor, N. Tirelli, J.A. Hubbell, Macromolecules 35 (2002) 8688–8693.
[32] A. Napoli, N. Tirelli, G. Kilcher, J.A. Hubbell, Macromolecules 34 (2001) 8913–8917.
[33] L. Wang, P. Hu, N. Tirelli, Polymer 50 (2009) 2863–2873.
[34] L. Wang, G. Kilcher, N. Tirelli, Macromol. Biosci. 7 (2007) 987–998.
[35] A. Napoli, M. Valentini, N. Tirelli, M. Muller, J.A. Hubbell, Nat. Mater. 3 (2004) 183–189.
[36] J.P. Bearinger, S. Terrettaz, R. Michel, N. Tirelli, H. Vogel, M. Textor, J.A. Hubbell, Nat. Mater. 2 (2003) 259–264.
[37] E.M. Di Meo, A. Di Crescenzo, D. Velluto, C.P. O'Neil, D. Demurtas, J.A. Hubbell, A. Fontana, Macromolecules 43 (2010) 3429–3437.
[38] M. Valentini, A. Napoli, N. Tirelli, J.A. Hubbell, Langmuir 19 (2003) 4852–4855.
[39] A. Napoli, M.J. Boerakker, N. Tirelli, R.J.M. Nolte, N. Sommerdijk, J.A. Hubbell, Langmuir 20 (2004) 3487–3491.
[40] D. Velluto, D. Demurtas, J.A. Hubbell, Mol. Pharmacol. 5 (2008) 632–642.
[41] A. Halperin, S. Alexander, Macromolecules 22 (1989) 2403–2412.
[42] E.A.G. Aniansson, S.N. Wall, M. Almgren, H. Hoffmann, I. Kielmann, W. Ulbricht, R. Zana, J. Lang, C. Tondre, J. Phys. Chem. 80 (1976) 905–922.
[43] R. Lund, L. Willner, D. Richter, E.E. Dormidontova, Macromolecules 39 (2006) 4566–4575.
[44] L. Willner, A. Poppe, J. Allgaier, M. Monkenbusch, D. Richter, Europhys. Lett. 55 (2001) 667–673.
[45] R. Lund, L. Willner, M. Monkenbusch, P. Panine, T. Narayanan, J. Colmenero, D. Richter, Phys. Rev. Lett. 102 (2009) 4.
[46] C. Honda, Y. Abe, T. Nose, Macromolecules 29 (1996) 6778–6785.
[47] E.E. Dormidontova, Macromolecules 32 (1999) 7630–7644.
[48] R. Pool, P.G. Bolhuis, Phys. Rev. Lett. 97 (2006) 4.
[49] A.G. Denkova, E. Mendes, M.O. Coppens, Soft Matter 6 (2010) 2351–2357.
[50] M.K. Johansson, R.M. Cook, Chem.-Eur. J. 9 (2003) 3466–3471.
[51] B.Y. Ren, F. Gao, Z. Tong, Y. Yan, Chem. Phys. Lett. 307 (1999) 55–61.
[52] V. Balzani, P. Ceroni, S. Gestermann, M. Gorka, C. Kauffmann, F. Vogtle, Tetrahedron 58 (2002) 629–637.
[53] M. Asano, F.M. Winnik, T. Yamashita, K. Horie, Macromolecules 28 (1995) 5861–5866.
[54] M. Miki, T. Kouyama, Biochemistry 33 (1994) 10171–10177.
[55] S.R. Stauffer, J.F. Hartwig, J. Am. Chem. Soc. 125 (2003) 6977–6985.
[56] W. Veatch, L. Stryer, J. Mol. Biol. 113 (1977) 89–102.
[57] L.G. Reddy, L.R. Jones, D.D. Thomas, Biochemistry 38 (1999) 3954–3962.
[58] R.A. Melnyk, A.W. Partridge, C.M. Deber, J. Mol. Biol. 315 (2002) 63–72.
[59] J.K. Lin, J.Y. Chang, Anal. Chem. 47 (1975) 1634–1638.
[60] D. Parkinson, J.D. Redshaw, Anal. Biochem. 141 (1984) 121–126.
[61] C. Cannizzo, S. Amigoni-Gerbier, M. Frigoli, C. Larpent, J. Polym. Sci. Polym. Chem. 46 (2008) 3375–3386.
[62] C. Sasaki, T. Hamada, H. Okumura, S. Maeda, J. Muranaka, A. Kuwae, K. Hanai, K.K. Kunimoto, Polym. Bull. 57 (2006) 747–756.
[63] L. Wang, G. Kilcher, N. Tirelli, Macromol. Chem. Phys. 210 (2009) 447–456.
[64] M. Morpurgo, F.M. Veronese, D. Kachensky, J.M. Harris, Bioconjucate Chem. 7 (1996) 363–368.
[65] M.P. Lutolf, J.A. Hubbell, Biomacromolecules 4 (2003) 713–722.
[66] S.C. Rizzi, J.A. Hubbell, Biomacromolecules 6 (2005) 1226–1238.
[67] S.P. Zustiak, J.B. Leach, Biomacromolecules 11 (2010) 1348–1357.
[68] J.W. Bae, E. Lee, K.M. Park, K.D. Park, Macromolecules 42 (2009) 3437–3442.
[69] G. Kilcher, L. Wang, N. Tirelli, J. Polym. Sci. Polym. Chem. 46 (2008) 2233–2249.